ELSEVIER

Journal of Alloys and Compounds 275–277 (1998) 76–80

Journal of ALLOYS AND COMPOUNDS

Arc-melting synthesis and crystal chemistry of $RT_2B_2(C)$ (R=rare earth, T=Rh, Co) compounds

Jinhua Ye[a,*], Toetsu Shishido[b], Takehiko Matsumoto[a], Tsuguo Fukuda[b]

[a]*National Research Institute for Metals, 1-2-1 Sengen, Tsukuba, Ibaraki 305, Japan*
[b]*Institute for Materials Research (IMR), Tohoku University, 2-1-1 Katahira-cho, Aoba-ku, Sendai 980, Japan*

Abstract

The effects of carbon content and rare earth size on the phase stability and crystal chemistry of $RT_2B_2(C)$ (R=rare earth, T=Rh, Co) compounds have been investigated using arc-melting synthesis and X-ray diffraction. It was found that, for the transition metal cobalt, $GdCo_2B_2C_x$ compounds could be obtained for x ranging from 0.0 to 1.0. The c-axis of the compound increases significantly with increase in carbon content, while the a-axis decreases slightly. For the transition metal rhodium, however, RRh_2B_2 could not be obtained for the largest lanthanide, La, or the smallest, Er. With the addition of C to the ternary system, new RRh_2B_2C compounds have been obtained for R=Y, La to Er, except Eu. The stability of the RRh_2B_2C phase decreases with decreasing lanthanide size, which can be explained from the rare earth dependence of the crystallographic parameters of the compounds. © 1998 Elsevier Science S.A.

Keywords: Arc-melting synthesis; Borocarbide; Crystal chemistry; X-ray diffraction

1. Introduction

R–T–B (R, rare earth; T, transition metal) ternary compounds have attracted wide interest for their superconducting and magnetic properties. Our group has studied the crystal growth, structure and physical properties of the system, especially of compounds with T=Co and Rh. We have grown single crystals of three ternary phases in R–Rh–B systems, such as RRh_3B, RRh_3B_2 and RRh_4B_4 [1–3]. However, the RRh_2B_2 compounds, which are readily synthesized for transition metals Co [4] and Fe [5], have not been obtained in spite of a great deal of effort.

Recently, in the system with carbon addition to the above-mentioned R–T–B ternary system, a new group of RT_2B_2C (T=Pd, Ni, Pt) compounds has been reported [6–8] and studied for their superconductivity at temperatures as high as the previous long-standing record of Nb_3Ge. The stability of RT_2B_2C compounds seems to depend strongly on the size of the rare earth and transition metal. It has been reported that RNi_2B_2C compounds can be obtained for lanthanides ranging from the largest, lanthanum, down to the smallest, lutetium [9]. For the larger transition metals Rh, Ir, Pd and Pt, however, only larger lanthanides are reported to form the RT_2B_2C phase. For the transition metals Co and Fe, which form RT_2B_2 ternary compounds for most lanthanide elements, very few quaternary compounds have been reported [10].

It is interesting that both the ternary and quaternary compounds crystallize in the $ThCr_2Si_2$-type structure [11]: intergrowth of tetrahedrally coordinated T_2B_2 layers with rare earth layers. The only difference between the two compounds is whether or not there is a C atom in the center of the rare earth layer, as can be expected from their chemical composition. It is therefore meaningful to elucidate the role of the C atoms in the crystal chemistry of the system, and the range of the solid solution of carbon in the system.

Recently, we studied the Rh-based quaternary system R–Rh–B–C and obtained several new RRh_2B_2C compounds [12]. As part of this work, we succeeded in growing single crystals of $GdRh_2B_2C$ [13] and reported its crystal structure [14]. In the present study, we focus our concerns on the relationship of the ternary RT_2B_2 and quaternary RT_2B_2C compounds, especially for the transition metals Co and Rh. We synthesized $GdCo_2B_2C_x$ compounds with x ranging from 0.0 to 1.0 using the arc-melting method. A quantitative understanding of the effects of the C content on the crystal chemistry of

*Corresponding author.

0925-8388/98/$19.00
PII: S0925-8388(98)00277-1

$RT_2B_2(C)$ systems was obtained. In addition, to elucidate the rare earth dependence of the phase stability of $RT_2B_2(C)$ compounds, we carried out a systematic study on the synthesis and characterization of $RRh_2B_2(C)$ compounds. Based on these results, a discussion on the controlling factors of the phase stability of $RT_2B_2(C)$ compounds is given.

2. Experimental

Samples were prepared by arc-melting and annealing. The starting materials were lanthanide metal (99.9%), Co powder (99.96%), Rh powder (99.9%), crystal boron (99.86%) and carbon powder (99.999%). For the synthesis of the $GdCo_2B_2C_x$ compounds, Gd, Co, B and C were mixed in the atomic ratio 1:2:2:*x*, where *x* was 0.0, 0.25, 0.5, 0.75 and 1.0, respectively. For Rh-based compounds, R, Rh, B and C were mixed in the atomic ratio 1:2:2:0 for synthesis of the RRh_2B_2 phase and 1:2:2:1 for RRh_2B_2C. To examine the size effects of the rare earth element on the crystal chemistry of the system, the largest La, medium Gd and smaller Er were selected for synthesis of RRh_2B_2. All lanthanides were used for RRh_2B_2C for more systematic research. The mixtures were arc-melted under a 1 atm argon atmosphere on a water-cooled copper hearth. The melted button was turned over and remelted three times to ensure homogeneity. The as-cast ingot was wrapped in tantalum foil and annealed in flowing He gas (200 ml min^{-1}) at 1475 K for 20 h.

X-ray powder diffraction was carried out on a rotating anode diffractometer using monochromatized Cu Kα radiation.

3. Results and discussion

3.1. Dependence of crystal chemistry on carbon content x in $GdCo_2B_2C_x$

Fig. 1 shows the X-ray diffraction pattern of the arc-melted $GdCo_2B_2C_x$ alloys, where *x* is (a) 0.0, (b) 0.25, (c) 0.5, (d) 0.75, and (e) 1.0. The chemical compositions of the alloys were analyzed using inductively coupled plasma atomic emission spectrometry (ICP) for Gd, Co and B. The combustion-infrared absorption method was applied for analysis of carbon. The results indicated that the Co and C contents of the arc-melted alloys were in a good agreement with the starting materials. However, Gd showed a slight increase (about 1.5%) and B showed an average decrease of 12% after arc-melting.

It can be seen from the diffraction patterns that arc-melted alloys of $GdCo_2B_2C_x$ with different *x* include a similar main phase, the diffraction peaks of which are indicated by circles in Fig. 1e. These peaks were identified as belonging to the diffractions of the $ThCr_2Si_2$-type structure. Except for this main phase, each of the arc-melted alloys with different carbon content contains some impurity phase, mainly $GdCo_3B_2$, indicated by triangles in Fig. 1a. With increasing carbon content, the peaks of the main phase become stronger, indicating not only the increase in the amount of the $GdCo_2B_2C_x$ phase obtained, but also a significant improvement in the crystallinity of the compounds. On the contrary, the greater the carbon content, the weaker the peaks of the impurity phase, i.e. the smaller the amount of $GdCo_3B_2$ phase formed. The diffraction patterns of the $GdCo_2B_2C_x$ phases were carefully indexed and the lattice parameters were evaluated from least-squares refinements of 2θ angles of more than 10 reflections ranging up to 100°. The carbon content dependencies of the *a*- and *c*-lattice parameters are plotted in Fig. 2a. It can be seen that the overall tendency with increasing carbon content is a slight decrease of the *a*-axis and a significant increase of the *c*-axis. As a result of the lattice parameter change, the unit cell volume of $GdCo_2B_2C_x$ compounds, shown in Fig. 2b, increases almost linearly as *x* increases from 0.0 to 1.0 (maximum 8.5%).

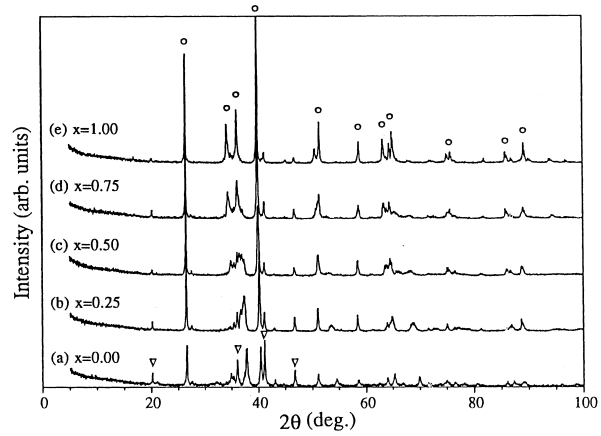

Fig. 1. X-ray diffraction patterns of arc-melted $GdCo_2B_2C_x$ compounds, where *x* is (a) 0.0, (b) 0.25, (c) 0.5, (d) 0.75 and (e) 1.0. Peaks indicated by circles in (e) belong to the $ThCr_2Si_2$-type structure; triangles in (a) are peaks of $GdCo_3B_2$.

Fig. 3 shows the structure of $GdCo_2B_2C_x$ compounds, a derivative of the $ThCr_2Si_2$-type. The rare earth R (=Gd), the transition metal T (=Co), B and C are represented by large open, medium shaded, small open, and small solid circles, respectively. The structure can be viewed as an intergrowth of RC NaCl-type layers and T_2B_2 layers. The difference between the structures of ternary RT_2B_2 and quaternary RT_2B_2C compounds therefore depends on whether or not there is a carbon atom in the center of the rare earth layer. The bonding of the inserted carbon with other atoms is illustrated as broken lines. In compounds

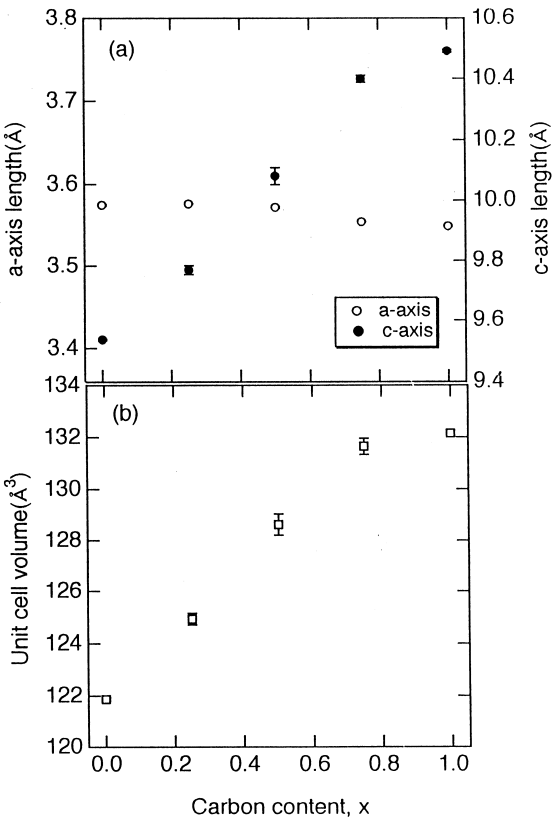

Fig. 2. Carbon content dependence of (a) the *a*-axis (○) and the *c*-axis (●); (b) unit cell volume of $GdCo_2B_2C_x$ compounds.

without carbon, the *c*-axis oriented layered structure is established by the boron–boron bonding. In compounds with carbon, the two layers are connected to each other by boron–carbon–boron bonding. The strong bonding between boron and carbon, as revealed in single crystals of $GdRh_2B_2C$ [14], seems to make it possible for the $ThCr_2Si_2$-type structure to accommodate a carbon content *x* from 0.0 to 1.0 in $GdCo_2B_2C_x$ compounds, while maintaining the overall structure unchanged.

From the crystal structure of $GdCo_2B_2C_x$ compounds, the increase of the *c*-axis with increasing carbon content is readily understood. With the insertion of carbon in the rare earth layer, the B–B atoms distributed along the *c*-axis must expand to allow insertion of the C atom, and to change the B–B bonding into B–C–B bonding. The slight decrease in the *a*-axis indicates contraction of the framework formed by the rare earth by the insertion of the carbon atom. This seems slightly incomprehensible. It may suggest strong bonding between the rare earth and carbon atom. It should be noted that the decrease in the *a*-axis with increasing carbon content from 0.0 to 1.0 is only 0.7%, which is negligibly small compared to the 10.0% increase in the *c*-axis.

A more systematic investigation of the effects of carbon content on the texture and physical properties of

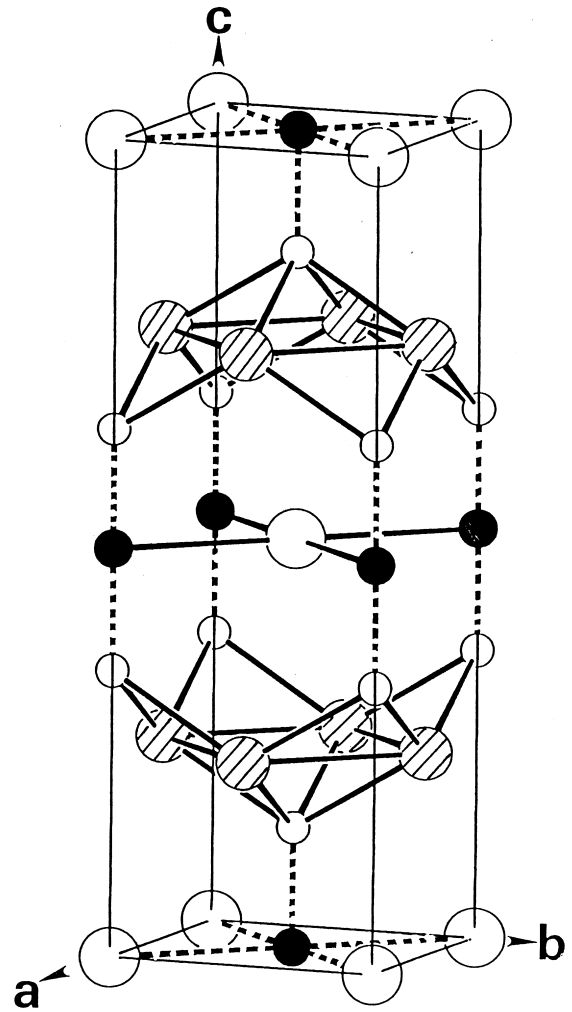

Fig. 3. Schematic diagram of the structure of RT_2B_2C (R=rare earth, T=transition metal). The R, T, B, and C atoms are represented as large open, medium shaded, small open, and small solid circles, respectively.

$GdCo_2B_2C_x$ compounds is in progress and the results will be published in a separate paper [15].

3.2. Dependence of crystal chemistry on rare earth size in $RRh_2B_2(C)$

X-ray diffraction of the Rh-based ternary alloys (R/Rh/B=1:2:2) revealed that for each lanthanide, the largest La, the medium Gd, and the smaller Er, the RRh_2B_2 phase was not formed. In the La–Rh–B system, LaB_6 and $LaRh_5$ were the main phases. In the case of the Gd- and Er-containing alloys, RRh_3B_2 was obtained as the main phase. This means that for the transition metal Rh, the RRh_2B_2 phase is difficult to form in a stable state for all rare earth elements.

Fig. 4 shows the X-ray diffraction patterns for the Rh-based quaternary alloys (R/Rh/B/C=1:2:2:1). A similarity in the main peak distribution of the diffraction patterns can be observed for lanthanides ranging from La

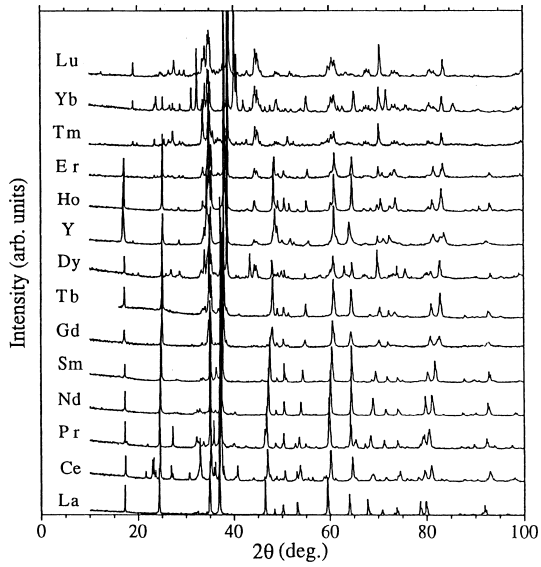

Fig. 4. X-ray diffraction patterns of the arc-melted materials with starting composition R/Rh/B/C=1:2:2:1 (R=La–Lu, Y).

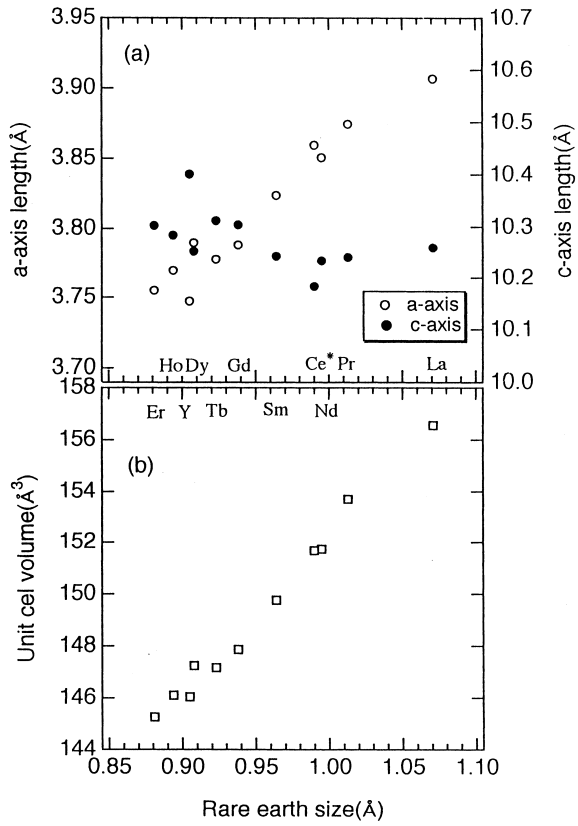

Fig. 5. Dependence of (a) the *a*-axis (○), the *c*-axis (●), and (b) the unit cell volume of RRh_2B_2C compounds on lanthanide size. Estimation errors are smaller than the symbols. The radius for Ce* is an assumed value corresponding to a valence of +3.4.

to Er, except Eu. The similar peaks were identified as belonging to the new borocarbides RRh_2B_2C, which crystallize in a modified structure of the $ThCr_2Si_2$-type. The lattice parameters of RRh_2B_2C were evaluated from least-squares refinements of the diffraction patterns. The *a*- and *c*-axes, and the unit cell volume of RRh_2B_2C compounds are plotted in Fig. 5a,b as a function of rare earth size as determined by Iandelli and Palenzona [16]. Only the radius of Ce was an assumed value (0.99 Å) corresponding to a valence of +3.4, which was estimated by interpolation of the unit cell volume of $CeRh_2B_2C$ to those of other rare earth compounds. The *a*- and *c*-axes data appear somewhat scattered. From the results obtained for the $GdCo_2B_2C_x$ compounds described in the last section, we consider that the scattering originates from the effects of carbon deficiency on the lattice parameters. As a general tendency, the tetragonal *a*-axis of RRh_2B_2C contracts as the size of the lanthanide decreases, in accordance with Vegard's law. The *c*-axis, however, shows a slight expansion. The variation is quite different from those reported for RNi_2B_2C [9], where the *c*-axis expands 7.3% from R=La to Er. The different behavior observed for Rh-based and Ni-based compounds implies significant effects of the transition metal on the crystal chemistry of the quaternary borocarbides.

As can be seen from Fig. 4, for lanthanide elements smaller than Tb, an impurity phase with a strong diffraction peak at 2θ of about 38.75° was observed. The impurity phase was identified to be RRh_3B_2. The RRh_3B_2 phase increases its volume ratio to RRh_2B_2C with decreasing rare earth size. For Tm, Yb and Lu, no RRh_2B_2C peaks could be observed, and the RRh_3B_2 phase becomes the main phase for the arc-melted alloys. A heat-treatment experiment was carried out on arc-melted alloys to examine the phase stability of RRh_2B_2C compounds. It was found that, when R=Er, after heating in an argon flow at 1400°C for 5 h, the polycrystal $ErRh_2B_2C$ decomposed, and only $ErRh_3B_2$ remained. For larger sized lanthanides, e.g. Nd or Gd, when annealed under the same conditions as above, the RRh_2B_2C compound did not decompose. Moreover, the X-ray diffraction peaks became sharper than before annealing. In the RRh_2B_2C group, R=Er is the smallest in size and seems, thermochemically, the most unstable.

For the tetragonal symmetry of the RRh_2B_2C compounds, the interatomic distances between the transition metals were easily calculated from the *a*-lattice parameter of the compounds (Rh–Rh $= a/\sqrt{2}$). As the *a*-axis decreases for the smaller lanthanide, the Rh–Rh distance also decreases significantly from 2.7623 Å in $LaRh_2B_2C$ to 2.6786 Å in $GdRh_2B_2C$, and further to 2.6552 Å in $ErRh_2B_2C$. The Rh–Rh distances in $GdRh_2B_2C$ and $ErRh_2B_2C$ are both shorter than the atomic distance (2.70 Å) expected from the metallic Rh radius [17]. The decreasing Rh–Rh distance explains the decreasing stability of RRh_2B_2C compounds for the smaller lanthanide atoms.

4. Conclusion

The crystal chemistry of $RT_2B_2(C)$ compounds was investigated for T=Co and Rh. It was found that for T=Co, the solid solution of carbon in $GdCo_2B_2C_x$ ranges from $x=0.0$ to 1.0. With increasing carbon content, the *c*-axis of the compounds increases significantly, reflecting expansion of the B–B bonding to B–C–B bonding along the *c*-axis. The *a*-axis, however, decreases slightly, suggesting strong bonding between the rare earth and carbon atom.

On the other hand, for T=Rh, no RT_2B_2 could be obtained, but RRh_2B_2C compounds were available in pure or multi-phase form for larger lanthanides ranging from La to Er (except Eu) and Y. The solid solution range of the carbon content in the $RRh_2B_2(C)$ system appears to be narrower than in $GdCo_2B_2(C)$. The stability of the RRh_2B_2C phase decreases with decreasing lanthanide size, which can be explained by the rare earth dependence of the crystallographic parameters of the compounds. The carbon content, size of the rare earth, as well as type of transition metal all seem to affect the stable formation and crystal chemistry of $RT_2B_2(C)$ compounds.

Acknowledgements

This work was performed under the Inter-university Cooperative Research Program of the Institute for Materials Research, Tohoku University. The authors are grateful to Messrs. K. Obara and T. Sugawara at IMR, Tohoku University, for assistance during sample preparation.

References

[1] T. Shishido, I. Higashi, H. Kitazawa, J. Bernhard, H. Takei, T. Fukuda, Jpn. J. Appl. Phys. 10 (1994) 142.
[2] T. Shishido, T. Sasaki, J. Ye, T. Fukuda, Bull. Chem. Soc. Jpn. 9 (1995) 703.
[3] T. Shishido, J. Ye, M. Oku, S. Okada, K. Kudou, T. Sasaki, T. Matsumoto, T. Fukuda, J. Alloys Comp. 248 (1997) 18.
[4] K. Niihara, T. Shishido, S. Yajima, Bull. Chem. Soc. Jpn. 4 (1973) 1137.
[5] G.F. Stepanchikova, Ju.B. Kuz'ma, B.I. Chernjak, Dopovidi Akad. Nauk Ukrains'koi Rsr Ser. A: Fiziko-Matematichni Ta Tekhnichni Nauki 40 (1978) 950.
[6] R.J. Cava, H. Takagi, B. Batlogg, H.W. Zandbergen, J.J. Krajewski, W.F. Peck Jr, R.B. Dover, R.J. Felder, T. Siegrist, K. Mizuhashi, J.O. Lee, H. Eisaki, S.A. Carter, S. Uchida, Nature 367 (1994) 146.
[7] R.J. Cava, H. Takagi, H.W. Zandbergen, J.J. Krajewski, W.F. Peck Jr., T. Siegrist, B. Batlogg, R.B. van Dover, R.J. Felder, K. Mizuhashi, J.O. Lee, H. Eisaki, S. Ushida, Nature 367 (1994) 252.
[8] R.J. Cava, B. Batlogg, T. Siegrist, J.J. Krajewski, W.F. Peck Jr., S. Carter, R.J. Felder, H. Takagi, R.B. van Dover, Phys. Rev. B 49 (1994) 12384.
[9] T. Siegrist, R.J. Cava, J.J. Krajewski, W.F. Peck Jr., J. Alloys Comp. 216 (1994) 135.
[10] F.M. Mulder, J.H.V.J. Brabers, R. Coehoorn, R.C. Thiel, K.H.J. Buschow, F.R. de Boer, J. Alloys Comp. 217 (1995) 118.
[11] Z. Ban, M. Sikirica, Acta Crystallogr. 18 (1965) 594.
[12] J. Ye, T. Shishido, T. Sasaki, T. Takahashi, K. Obara, R. Note, T. Matsumoto, T. Fukuda, J. Solid State Chem. (in press).
[13] T. Shishido, J. Ye, T. Sasaki, R. Note, K. Obara, T. Takahashi, T. Matsumoto, T. Fukuda, J. Solid State Chem. (in press).
[14] J. Ye, T. Shishido, T. Kimura, T. Matsumoto, T. Fukuda, Acta Crystallogr. C 52 (1996) 2652.
[15] T. Shishido, J. Ye, K. Obara, T. Fukuda, J. Ceram. Soc. Jpn. (submitted).
[16] A. Iandelli, A. Palenzona, in: K.A. Gschneider, L. Eyring (Eds.), Handbook on the Physics and Chemistry of Rare Earths, Vol. 2, North-Holland, Amsterdam, 1984, chapt. 13.
[17] W.B. Pearson, in: The Crystal Chemistry and Physics of Metals and Alloys, Wiley, New York, 1972.